Food and Bioprocess Technology
https://doi.org/10.1007/s11947-018-2097-2

ORIGINAL PAPER

A New Chemical Marker-Model Food System for Heating Pattern Determination of Microwave-Assisted Pasteurization Processes

Jungang Wang[1] · Juming Tang[1] · Frank Liu[1] · Stewart Bohnet[1]

Received: 10 August 2017 / Accepted: 15 March 2018

Abstract

New chemical marker-model food systems with D-ribose and NaOH precursors as color indicators and gellan gels as chemical marker carrier were explored for the assessment of the heating pattern of in packaged foods processed in microwave-assisted pasteurization system (MAPS). In determining appropriate precursor concentrations, a solution of 2% (*w*/*w*) D-ribose and 60 mM NaOH was heated at 60–90 °C for 0–20 min. The solution absorbance at 420 nm increased linearly, while the color parameters L^* decreased linearly with heating time at all processing temperatures. In storage, the produced brown color was stable at 4 and 22 °C within 7 days. The new chemical marker-model foods were prepared by mixing 2% (*w*/*w*) D-ribose and 60 mM NaOH with 1% (*w*/*v*) low-acyl gellan gum and 20 mM $CaCl_2 \cdot 2H_2O$ solution. The dielectric constant of the model food samples decreased with the addition of sucrose, and the loss factors increased with the addition of salt. After processing in the pilot MAPS, the heating pattern and cold and hot spots in the new chemical marker-model food system could be clearly recognized and precisely located through a computer vision method. This is the first time that the caramelization reaction was used as a time-temperature indicator in gellan gel model food. This study shows the possibility of using the new chemical marker-model food system for heating pattern determination of the MAPS.

Keywords Microwave-assisted pasteurization system (MAPS) · Chemical marker · Caramelization · Gel model food · Heating pattern

Introduction

Thermal processing has been used since the nineteenth century in the food industry to produce shelf-stable food products (Thorne 1986). The main purpose of a thermal process is to inactivate pathogenic and spoilage microorganisms; however, the quality of food products may also be lost due to long time heating at high temperatures. One effective measure to reduce the thermal damage is to shorten the heating time (Richardson 2001). Microwave-assisted thermal processing as a novel food processing technology can significantly reduce processing time and provide better food quality (Lau and Tang 2002; Tang 2015).

✉ Juming Tang
Jtang@wsu.edu

[1] Department of Biological Systems Engineering, Washington State University, PO Box 646120, 1935 E. Grimes Way, Pullman, WA 99164-6120, USA

A major challenge of microwave-assisted thermal processing is non-uniform heating. To ensure the safety of packaged foods, the cold spot must be located for process development. Kim and Taub at the US Army Natick Research Center identified three chemical markers: 2,3-dihydro-3,5-dihydroxy-6-methyl-(4H)-pyran-4-one(M-1), 4-hydroxy-5-methy-3(2H)-furanone(M-2), and 5-hydroxymethylfurfural(M-3) based on the Maillard browning reactions to estimate non-uniform temperature distribution and for cold spot determination (Kim and Taub 1993). The method provided kinetic relationships between chemical marker yields and time-temperature influences, so the corresponding processing extent could be estimated by quantifying the marker yield. Pandit et al. (2007a) improved the heating pattern determination method by correlating quantified color value on gray scale, with thermal lethality F_0 and marker yield. By doing so, the heating pattern can be analyzed through a computer vision system (CVS) method, thus largely reducing the cost and analyses time. Among the three chemical markers, M-2 was the most widely used for high temperature short-time (HTST) processes (Kim et al. 1996; Lau et al. 2003; Prakash et al. 1997).

Published online: 28 March 2018

Researchers at Washington State University developed 915 MHz microwave-assisted thermal sterilization (MATS) technology for production of shelf-stable low acid foods and 915 MHz microwave-assisted thermal pasteurization systems (MAPS) for chilled foods. Typical target process temperatures for MATS are 120–130 °C and for MAPS are 70–90 °C (Tang 2015). M-2 has been used in MATS (Pandit et al. 2007b) for heating pattern determination. Mashed potato and D-ribose were applied to produce M-2 with processing temperatures exceeding 110 °C (Pandit et al. 2006). D-Ribose and L-Lysine were highly recommended as the reactants to produce M-2 due to their high efficiency of the Maillard browning reaction (Ashoor and Zent 1984). However, the L-Lysine (L5501, Sigma, USA) used in the heating pattern determination in MAPS has limited industry application due to its high price. Also, the formation of M-2 needs a relatively high temperature; thus, it can hardly be produced in the pasteurization temperature range from 60 to 100 °C (Zhang et al. 2014). Therefore, other chemical markers with low cost and high sensitivity need to be developed for industrial utilization of MAPS. Caramelization, as a non-enzymatic reaction, can also produce brown color. Unlike the Maillard reaction, there is no amino acid participated in the caramelization reaction, which largely reduces the cost. Also, the reaction can be catalyzed by acidic and alkaline conditions, so the reaction rate can be promoted by adjusting the pH of the solutions (Namiki 1988).

A main function of a model food is to serve as a carrier of chemical markers in the heating pattern determination for microwave-assisted thermal processes. In MATS, mashed potato and whey protein gel model foods were developed as carriers for chemical marker formation (Pandit et al. 2006; Wang et al. 2004). Computer simulation and experimental results for MATS systems indicated that the cold spot was located in the middle of the processed samples (Resurreccion et al. 2013; Tang et al. 2008); thus, the model food should be capable of being cut into different layers, and then the color change in the middle layer was used for heating pattern analyses. The soft mashed potato model foods cannot provide a texture for cutting into different layers, thus largely limiting its application. Whey protein gel model foods, on the other hand, form a steady gel with appropriate texture for cutting and color analyses. Whey protein gels have been applied extensively as the model food for heating pattern determination in MATS, and the results for the middle layer were used to develop protocols to file for FDA acceptance (Tang 2015). The whey protein gels used for heating pattern determination in MATS were usually prepared with whey protein 20 g/100 g wet basis. Such whey protein model food systems need to be heated at 80 °C for 40 min before forming a firm and uniform gel (Lau et al. 2003; Wang et al. 2004). For heating pattern determination in MAPS, the chemical marker should be able to produce different levels of color with different processing intensity for temperature range from 70 to 90 °C. Temperature at 80 °C is too high for chemical marker-model food system for MAPS since the chemical marker will change the color before forming a gel. Such changes could lead to inaccurate evaluation of the heating pattern after the microwave-assisted thermal processing.

Zhang et al. (2013, 2015) studied the application of egg white and gellan gel for MAPS and recommended gellan gels as model foods for heating pattern determination. Gellan is a water-soluble anionic extracellular polysaccharide produced by the bacterium *Sphingomonas elodea* known as *Pseudomonas elodea* (Pollock 1993). Gellan gel has the advantages of high gelation efficiency, good thermal stability, and a wide range of mechanical properties (Morris et al. 2012). Native gellan polysaccharide is a high acyl form due to the existence of L-glyceryl and acetyl groups (Kuo et al. 1986). After processing by alkali at high temperature, the substitutes were removed, processing the low-acyl gellan. The gellan gel formed by low-acyl gellan is firm and clear (Tang et al. 1994, 1995, 2001); the gelation temperatures can be adjusted from 40 to 70 °C with different polymer and cation concentrations (Tang et al. 1997a, b). Therefore, low-acyl gellan is preferred in preparation of the model foods for heating pattern determination in MAPS.

The objective of this study was to explore the possibility of using the caramelization reaction to produce a chemical marker as the time-temperature indicator in low-acyl gellan gel model foods for heating pattern determination of microwave-assisted pasteurization processes. This study consisted of two parts: (1) investigating color formation and stability in selected solutions with appropriate color precursors and (2) developing gel models that incorporated the selected solutions for color formation in solid matrices. The color changes and stability of the chemical marker were detected by the color parameter L^* and absorbance. Physical properties (dielectric properties, penetration depth, and texture) of the chemical marker-model food system were determined to evaluate its feasibility for microwave heating. The heating pattern of the new chemical marker-model food system was detected; cold and hot spots in 10.5 oz trays were located using the computer vision method after being processed in the pilot MAPS. Lastly, a mobile temperature sensor determination was conducted to validate the obtained heating patterns.

Materials and Methods

Sample Preparation

Solutions of D-ribose and NaOH were prepared by slowly adding 2% (*w*/*w*) D-ribose and 60 mM NaOH into double-deionized (DDI) water at 22 °C; the solution was stirred

on a magnetic stirrer until D-ribose was completely dissolved. The pH of the final solution was 12.

Gellan solutions were prepared by slowly adding 1% (*w*/*v*) low-acyl gellan gum (CP Kelco Inc. Atlanta, GA) into DDI water at 22 °C; the mixtures were stirred on a magnetic stirrer for 1 h, and then slowly heated to 90 °C. Twenty mM $CaCl_2 \cdot 2H_2O$ and 2% (*w*/*w*) D-ribose were added into the solution at 90 °C; the solutions were cooled down to 60 °C. NaOH was added at 60 °C, and the solutions were continually stirred for 1 min to obtain a final NaOH concentration of 60 mM.

Water Bath Treatment

The kinetics of color change in solutions during thermal treatments is important to estimate the corresponding color for a given temperature-time history. The kinetic studies were conducted under isothermal conditions. The thermal influence during the come-up time (the time that samples reached 0.5 °C below the set temperature) should be reduced or eliminated to the greatest extent (Chung et al. 2007). In this study, custom-built aluminum thermal kinetics testing (TKT) cells designed at Washington State University (Zhang et al. 2014) were used. The heating time was considered to start at the end of the come-up time, which in this study was around 30 to 50 s. TKT cells, each containing 5 mL of 2% (*w*/*w*) D-ribose and 60 mM NaOH solution, were heated in a water bath (Model HAAKE DC 30, Thermo Electron Corp., Waltham, MA, USA) at 60, 70, 80, and 90 °C for 0, 2, 5, 7, 10, 15, and 20 min. After heating, the TKT cells were cooled immediately in ice water for 3 min, then equilibrated to room temperature before color value measurement.

Color Value Determination

After the heat treatment, the color parameter L^* (Lightless) of the samples was measured by CVS and CS6 Photoshop Software (Adobe system, Inc., San Jose, CA) as described in Zhang et al. (2014). Wavelength at 420 nm was recommended for the measurement of the yellow and brown color (Levinson 2001). Thus, the absorbance of samples at 420 nm was determined using a Shimadzu UV-2550 spectrophotometer (Shimadzu Co, Kyoto, Japan) for the evaluation of color change. All measurements were conducted in triplicate.

Color Stability

Solutions of D-ribose and NaOH were heated in a water bath at 80 °C for 5, 10, 15, and 20 min to study the influences of storage time on the color stability. The processed samples were sealed in 15-mL centrifuge tubes and covered with aluminum foil to eliminate the effects of light. Samples were stored at 4 and 22 °C, and L^* and pH were measured on storage times 0, 1, 3, 5, and 7 days. The pH was measured by pH meter (AP5, Fisher Scientific International, Inc, New Hampshire, USA). All measurements were conducted in triplicate.

Dielectric Properties Measurement

The dielectric constant (the ability to store electric energy, ε') and the loss factor (the ability to dissipate the electrical energy into heat, ε'') are the two most important dielectric properties of food, which are used to evaluate the thermal behavior of food materials in microwave heating. At room temperature, the dielectric constant and loss factor of most fruits and vegetables ranged from around 60 to 80 and 10 to 30 respectively, at 915 MHz (Venkatesh and Raghavan 2004; Wang et al. 2003a, 2005). The dielectric properties of meats vary due to their different composition, but for the most common meats such as raw beef, chicken, and turkey, the dielectric constant and loss factor are around 60 and 30 at 915 MHz (To et al. 1974; Tran and Stuchly 1987). For an ideal model food system, it should have the flexibility to cover a wide range of dielectric constant and loss factors to match those of real foods. In the current study, we added salt to adjust the loss factor and sucrose to adjust the dielectric constant (Luan et al. 2015b) of the new chemical marker-model food system.

In addition to the gelation solution steps described in the "*Sample preparation*" section, salt and sucrose were added at 90 °C so that the solutions consisted of 0, 100, 200, and 300 mM salt and 0, 0.1, 0.2, 0.3, and 0.4 g/mL sucrose. The solutions were poured into 50-mL plastic centrifuge tubes and cooled down in a refrigerator (4 °C) to set the gels. An HP 8752 C network analyzer with 85070B open-end coaxial dielectric probe (Agilent Technologies, Santa Clara, CA, USA) as described in Guan et al. (2004) was used to measure the dielectric properties. Gel samples were cut into a cylindrical shape with a diameter of 20 mm by using a steel tube with sharp edges. The samples were then placed in the testing cell with an inner diameter of 21 mm and a height of 94 mm; the testing cell was heated in a circulating oil bath up to 100 °C, while the corresponding dielectric constant and dielectric loss factor were measured at every 10 °C increments over the temperature range of 20 to 100 °C. Detailed information of the testing cell is described in Wang et al. (2003b). The testing cell was cooled down to a temperature lower than 20 °C using a programmable circulator (1157, VWR Science Products, Radnor, PA, USA) and cleaned thoroughly before the next measurement. All measurements were conducted in duplicate.

Penetration Depth

Information on penetration depth of the microwave in foods is important for designing the size, especially the thickness, of the packaged foods in microwave-assisted thermal processes. It is defined as the depth where the incident power decreased to 1/e (Euler's number e ≈ 2.718) of the power entering the material's surface (Von Hippel 1995) and is calculated from:

$$D_p = \frac{c}{2\pi f\sqrt{2\varepsilon'\left[\sqrt{\left(\frac{\varepsilon''}{\varepsilon'}\right)^2+1}-1\right]}} \quad (1)$$

where c is the speed of light in free space (3×10^8 m/s), and f is the frequency, which in this study is 915 MHz (915,000,000 Hz).

Gel Model Texture Measurement

Different predetermined amounts of low-acyl gellan were added to make final gellan gum concentrations of 0.5, 1 and 1.5% (*w*/*v*), and $CaCl_2 \cdot 2H_2O$ was added when solutions reached 90 °C to make final $CaCl_2 \cdot 2H_2O$ concentrations of 5, 10, 20, and 40 mM. The solution samples in 50 mL plastic centrifuge tubes were cooled down in a refrigerator (4 °C) to set the gels. Gel samples were then cut into a cylindrical shape with a diameter of 20 mm and a height of 20 mm using a steel tube with sharp edges. The texture measurements were conducted using the TA-XT2i Texture Analyzer (Texture Technologies Corp, Scarsdale, NY) with a 25 mm diameter aluminum cylinder probe. The contacted surfaces of the samples were lubricated and compressed to failure with a testing speed of 1 mm/s. The maximum force (F_{max}) and deformation (ΔL_{max}) were recorded for the true gel stress (σmax) and gel strain (εmax) calculation (Hamann 1983):

$$\varepsilon_{max} = -\ln\left[1-\frac{\Delta L_{max}}{L}\right] \quad (2)$$

$$\sigma_{max} = \frac{F_{max}(L-\Delta L_{max})}{\pi R^2 L} \quad (3)$$

where L and R are the original height and radius of the gel samples. For the cylindrical gel model food, a shear mode was observed in gellan gels during the compression testing; thus, the shear strain (γ_{max}) which represents the extensibility and shear stress (τ_{max}) which represents the strength at failure were calculated by the following equations to represent the true failure properties of the gel model food (Tang et al. 1994):

$$\gamma_{max} = (1+\nu)\varepsilon_{max} \quad (4)$$

$$\tau_{max} = \frac{\sigma_{max}}{2} \quad (5)$$

where the Possion's ratio ν was set as 0.5 (Juvinall 1967). Six replicates were conducted for each measurement.

Microwave-Assisted Pasteurization Process

A pilot-scale single-mode (915 MHz) microwave-assisted pasteurization system developed at Washington State University (Fig. 1) was used in this study. By adjusting the microwave power and conveyor speed, the MAPS can raise the temperature of different food products to between 70 and 90 °C within a short time (1.5 to 2 min) to inactivate pathogenic bacteria and viruses (Tang 2015).

Gellan solution (10 oz) was poured into plastic trays (14 cm × 9.5 cm × 3 cm) and cooled down in a refrigerator

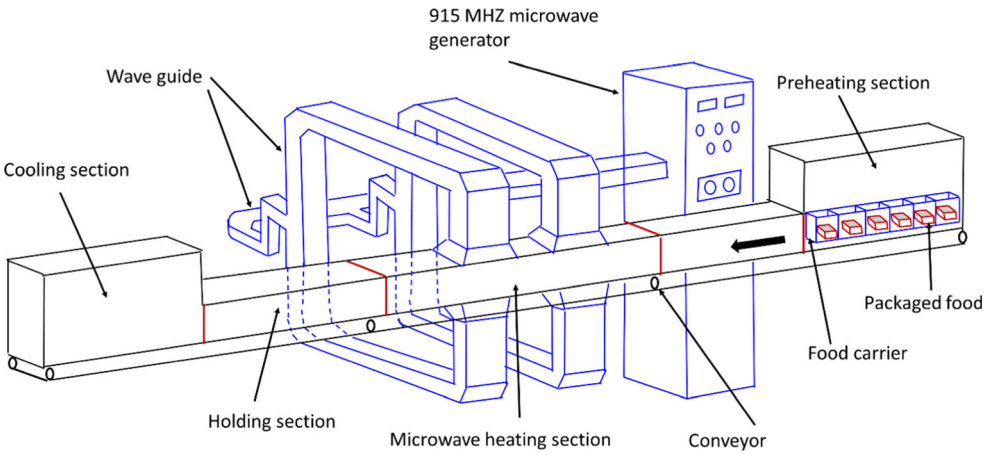

Fig. 1 Microwave-assisted pasteurization system (MAPS) diagram

(4 °C) to set the gels. Samples were then vacuum-sealed and equilibrated to room temperature before processing in MAPS. The MAPS consisted of four sections: preheating, microwave heating, holding, and cooling. Samples were placed in a tray carrier and pre-heated in the preheating section for 30 min with a water temperature of 60 °C, then moved through (at 25 in/min) the microwave heating section where 5 kW of microwave power was applied to both cavities to allow a rapid increase of sample temperature. Water immersion was applied during the microwave heating process to reduce edge heating (Tang 2015). After that, the samples were moved to the holding section and held for 6 min with circulating water at 90 °C, followed by a 5-min cool down in the cooling section with a water temperature of 25 °C. Following this, the samples were unloaded from the MAPS for heating pattern determination.

Heating Pattern Determination and Validation

After processing by the MAPS, the gel model foods were unloaded and cut horizontally along the middle plane. Since the gellan gel model foods are transparent, the color at the bottom could influence the accuracy of the heating pattern determination; a layer of 5 mm thickness was cut horizontally below the mid line to minimize the influence of the bottom color. Images of the cut layers were taken from CVS, and the heating patterns were analyzed by CS6 Photoshop software (Adobe system, Inc., San Jose, CA) and IMAQ vision builder (National Instrument Product, Austin, TX) with a script designed by Pandit et al. (2007a).

Validation of the heating pattern was conducted by using TMI mobile metallic temperature sensors (TMI-USA Inc., Reston, VA, USA), which has been proven to be a reliable and accurate method in microwave heating processes (Luan et al. 2013, 2015a). The location of the cold and hot spots was determined by comparing the average value of the prominent temperature zones. After locating cold and hot spot locations, the mobile metallic sensors with a protective metal tube (diameter 2 mm, length 50 mm) were horizontally inserted into the middle layer of the gel samples, and placed with the measuring point of the sensors at the location of the cold and hot spots. Temperature profiles were generated after analyzing the temperature changes recorded by the mobile metallic sensor during the MAPS process.

Data Analyses

The kinetic model of color change during heat treatment can be described using Eqs. 6–8, which were derived from Espenson (1995):

$$\text{Zero order}: C_t = C_0 - kt \tag{6}$$

$$\text{First order}: \ln\frac{C_t}{C_0} = C_0 - kt \tag{7}$$

$$\text{Second order}: \text{kt} = \frac{1}{C_t} - \frac{1}{C_0} \tag{8}$$

where C_0 is the color value at time zero, C_t is the color value at time t and k is the reaction rate constant.

If the color reached an equilibrium status after long time heating, then the fractional conversion model based on first-order kinetics can be used to describe the reaction (Rizvi and Tong 1997):

$$\text{f} = \frac{C_0 - C_t}{C_0 - C_\infty} \tag{9}$$

$$\ln(1-\text{f}) = \ln\left(\frac{C_t - C_\infty}{C_0 - C_\infty}\right) = -kt \tag{10}$$

where f is the color change index, C_0 is the initial color value, C_t is the color value at time t, and C_∞ is the color value after prolonged heating time.

Statistical analyses were conducted by using SAS (SAS Institute Inc., Cary, NC, USA). Differences between group means were analyzed by Tukey's multiple-range test. Statistical significance level P was set at 0.05 probability level.

Results and Discussion

Color Changes in Thermal Treatment

As a non-enzymatic reaction, the caramelization browning is greatly influenced by temperature, time, and pH (Ajandouz et al. 2001, 2008). In this study, the L^* and absorbance were used to obtain the relationship between brown color changes in ribose-NaOH solutions with an initial pH of 12 and processing time at different temperatures. In the L/a/ b color system, L^* stands for the luminance or lightness component of the samples (Leon et al. 2006), which quantifies the color changes of different levels of brown color. As indicated in Fig. 2a, L^* of ribose-NaOH solutions decreased with increasing processing time at all the tested temperatures. First reaction order kinetics were obtained between L^* and processing time, with R^2 (coefficient) ranging from 96.7 to 98.9%. Absorbance at 420 nm of ribose-NaOH solutions increased with increasing processing time (Fig. 2b). The increasing rates of absorbance were consistent at 60 and 70 °C. However, the increasing rates of absorbance in the early phase (0–10 min) were much higher than in the later phase (10-20 min) at 80 and

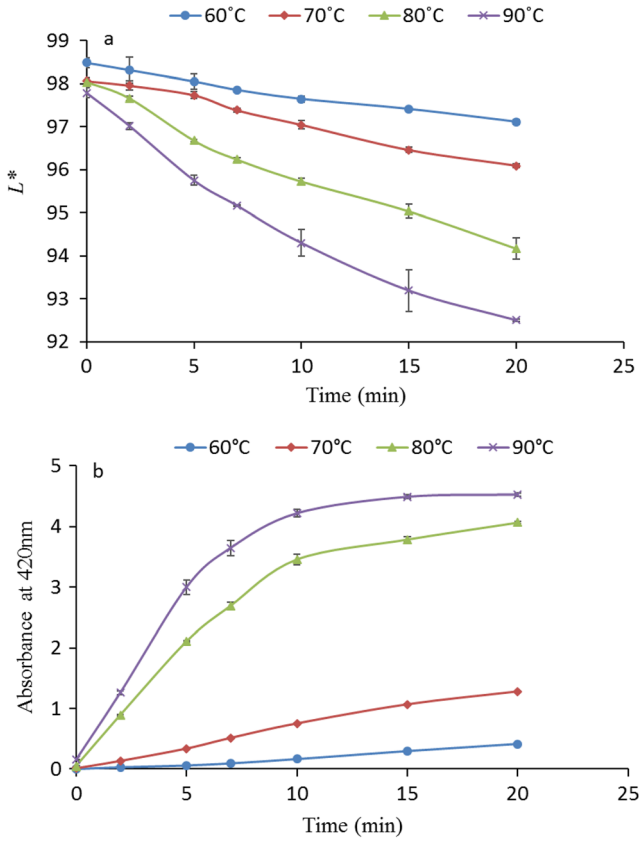

Fig. 2 L^* (**a**) and absorbance at 420 nm (**b**) of ribose-NaOH solutions after heat treatments; mean ± SD for three determinations

90 °C; thus, fractional conversion model which is usually used to describe two or more different phases of the reaction (Zimeri and Tong 1999) was applied in this study. The equilibrium status of the brown color was achieved by heating solutions for 120 min. The equilibrium absorbance values of solution at 60, 70, 80, and 90 °C were 2.64, 3.90, 4.43, and 4.54, respectively. Fractional first-order kinetics were obtained between absorbance and processing time with R^2 97.5, 99.6, 98.9, and 99.1% of 60, 70, 80, and 90 °C. However, compared to the fractional first order, zero-order kinetics ($R^2 = 98.04$) can better describe the color absorbance at 60 °C. We believe that the absorbance of the brown color at all temperatures would eventually follow fractional first order if we continue to extend the thermal treatment time. Similar color change trends were found by Ajandouz and Puigserver (1999) and Ajandouz et al. (2001) on the caramelization browning of glucose and fructose with solution pH at 12.

Both the L^* and absorbance indicated that the higher the processing temperature and longer heating time, the higher the brown intensity. But the color changes as indicated by L^* followed the first order at all processing temperatures, which is similar to the inactivation kinetics of microorganisms (Stumbo 1965). Thus, the L^* provided a more apropos relationship compared to absorbance at 420 nm.

Color Stability after Thermal Treatment

In our previous studies using chemical marker to determine the heating patterning of microwave-assisted sterilization processes, the produced brown color remained stable after the thermal process. Thus, the measurement of color in different locations of a model food truly reflected heating pattern in a MATS process. For the new chemical marker-model food system that we are elevating for the microwave-assisted pasteurization system, it is also desirable to maintain stable colors after thermal processing to reflect the heating patterns. Thus, it was necessary to study the stability of color in solution after thermal treatments.

The color stability of the samples after being heated at 80 °C was evaluated over 7 days at 4 °C and 22 °C by measuring the L^* of ribose-NaOH solutions. Significant differences ($p < 0.05$) were found in the L^* (mostly decreased) with the prolonged storage time at 4 and 22 °C, which indicated that more brown color was produced during storage (Table 1). No significant difference was found in the L^* between samples after the same heat treatments but stored at 4 and 22 °C. Thus, the storage time had more influences on the L^* than the storage temperature. Similar results can be concluded from the change of pH values. During the storage, the pH of solution decreased with the prolonged storage time, which indicated that the caramelization reaction continued during storage. The pH changes of processed solutions at 22 °C were higher than 4 °C with the prolonged storage time, which indicated higher reaction rates at 22 °C storage temperature. However, such differences in the reaction rate could not result in significant differences in the L^* values within 7 days of storage.

It has been reported that the caramelization browning reaction rate increased in a high alkaline condition (10–12) (Kim and Lee 2008; Namiki 1988). The results of this study indicated that the ribose-NaOH solutions still produced brown color at a temperature as low as 4 °C. Consequently, more accurate results for heating pattern determination could be achieved by storing the treated samples for shorter storage time before analyses. Nevertheless, the maximum change of L^* was less than 2% over 7-day storage, which is in agreement with the previous study of Kamuf et al. (2003) that the caramelization reaction rate was relatively low at ambient storage temperature. The caramelization brown color can be considered stable at both 4 and 22 °C within 7 days.

Effect of Salt and Sucrose on Dielectric Properties

Dielectric constant decreased with increasing temperature, but no significant differences ($p > 0.05$) were observed after adding 100, 200, and 300 mM salt (Fig. 3a). This indicates that there was a limited effect of salt on the dielectric constant of the new chemical marker-model food system. The dielectric constant, however, significantly decreased after adding 0.1,

Table 1 L^* and pH of heated ribose-NaOH solution during storage at 4 and 22 °C; mean ± SD for three determinations

Storage temp (°C)	Storage time (day)	Heating time							
		5 min		10 min		15 min		20 min	
		pH	L^*	pH	L^*	pH	L^*	pH	L^*
4	0	11.45 ± 0.01	96.42 ± 0.08^{a}	10.95 ± 0.05	95.48 ± 0.10^{a}	10.28 ± 0.01	94.80 ± 0.22^{a}	9.52 ± 0.04	94.05 ± 0.13^{a}
	1	11.34 ± 0.01	96.76 ± 0.06^{ab}	10.77 ± 0.01	95.62 ± 0.05^{a}	9.85 ± 0.01	94.43 ± 0.33^{ab}	9.12 ± 0.08	93.59 ± 0.21^{ab}
	3	11.11 ± 0.03	97.52 ± 0.16^{b}	10.00 ± 0.02	95.28 ± 0.08^{a}	8.41 ± 0.01	94.07 ± 0.23^{b}	8.13 ± 0.05	93.56 ± 0.39^{ab}
	5	10.82 ± 0.02	97.59 ± 0.02^{b}	9.46 ± 0.03	95.18 ± 0.10^{a}	8.12 ± 0.01	93.70 ± 0.08^{bc}	7.86 ± 0.01	92.98 ± 0.07^{b}
	7	10.48 ± 0.02	96.80 ± 0.80^{ab}	8.84 ± 0.02	94.44 ± 0.51^{b}	7.83 ± 0.01	93.45 ± 0.07^{c}	7.62 ± 0.01	93.01 ± 0.45^{b}
22	0	11.46 ± 0.01	96.69 ± 0.02^{a}	10.81 ± 0.02	95.71 ± 0.06^{a}	10.11 ± 0.01	95.14 ± 0.14^{a}	9.47 ± 0.03	94.13 ± 0.02^{a}
	1	11.16 ± 0.01	96.56 ± 0.09^{a}	10.28 ± 0.02	95.52 ± 0.02^{a}	9.30 ± 0.04	94.84 ± 0.15^{a}	8.68 ± 0.01	94.07 ± 0.19^{a}
	3	10.41 ± 0.03	96.50 ± 0.06^{ac}	8.31 ± 0.04	94.82 ± 0.17^{b}	7.62 ± 0.02	93.73 ± 0.11^{b}	7.33 ± 0.03	92.52 ± 0.18^{b}
	5	9.50 ± 0.01	96.24 ± 0.10^{bc}	7.70 ± 0.06	94.21 ± 0.23^{c}	7.22 ± 0.02	93.48 ± 0.06^{bc}	7.03 ± 0.02	92.50 ± 0.09^{b}
	7	8.19 ± 0.01	96.29 ± 0.14^{c}	7.28 ± 0.04	94.24 ± 0.10^{c}	7.02 ± 0.03	93.35 ± 0.06^{c}	6.88 ± 0.04	92.84 ± 0.28^{b}

Values with different letters in the same column are significantly different (P<0.05)

0.2, 0.3, and 0.4 g/mL sucrose (Fig. 3c), which is in reasonable agreement with other studies (Guan et al. 2004; Stogryn 1971; Zhang et al. 2015). Morris et al. (2012) explained that the sugar-water association was formed after adding sucrose into solution, which reduced the content of free water and resulted in a decrease of dielectric constant. The dielectric loss factor of the new chemical marker-model food system significantly increased with increasing salt content (Fig. 3b). A decreasing trend was observed for the dielectric loss factor when increasing the sucrose content (Fig. 3d). Thus, the dielectric loss factor was adjustable by controlling the content of salt and sucrose. However, the influences of salt content on dielectric loss factor were prominent compared to sucrose content. Therefore, adjusting the content of salt was preferred for a targeted dielectric loss factor.

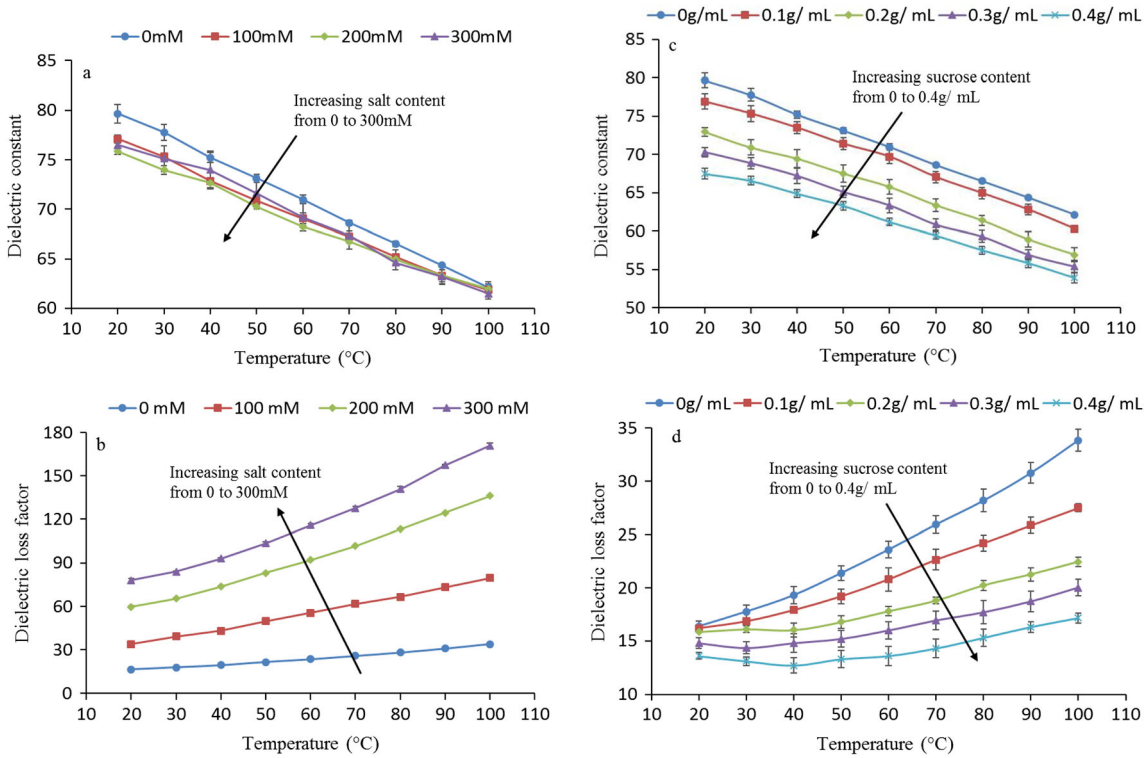

Fig. 3 The effect of salt (**a**, **b**) and sucrose (**c**, **d**) on the properties of new model food at 915 MHz between 22 and 100 °C; mean ± SD for two determinations

Generally, different food materials could achieve similar thermal treatment intensities in dielectric heating if their dielectric and thermal properties are similar (Ryynänen 1995). At room temperature, the dielectric constant and loss factor of the new chemical marker-model food system could range from approximately 65 to 80 and 15 to 80 at 915 MHz by adjusting the sucrose and salt content respectively. Thus, the model food can cover a wide range of the dielectric properties of the real foods, which allows the model food to more accurately simulate the thermal behavior of different food materials.

Effect of Salt and Sucrose on Penetration Depth

Compared to the 2450 MHz microwaves, a lower frequency of 915 MHz has deeper penetration depth, which provides the potential of more uniform heating in microwave thermal treatment. The penetration depth of 915 MHz microwaves in the new chemical marker-model food system decreased with increasing temperature (Fig. 4), which can be attributed to the increasing loss factor and decreasing dielectric constant with the increasing temperature.

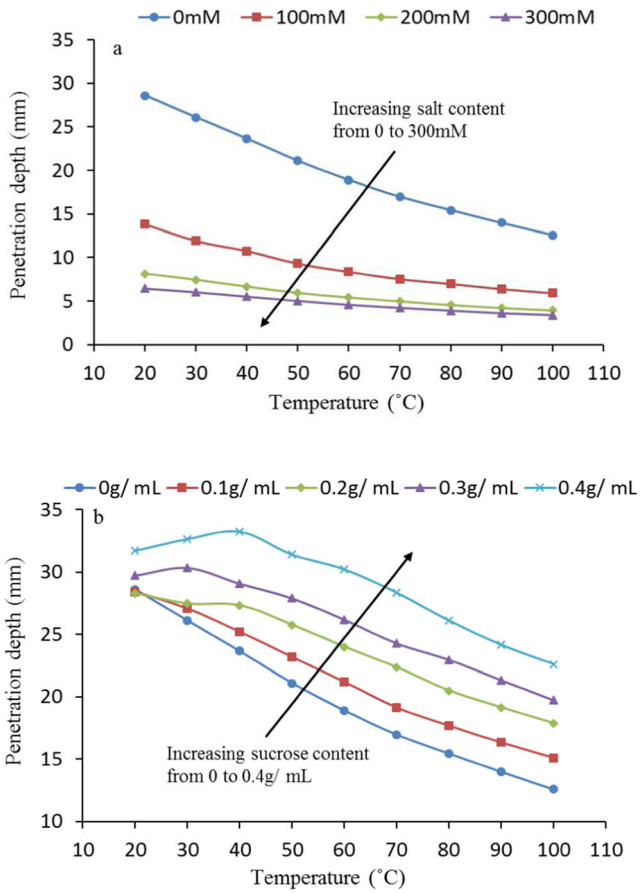

Fig. 4 Effect of salt (**a**) and sucrose (**b**) on penetration depth of new model food at 915 MHz between 22 and 100 °C

Penetration depths of the new chemical marker-model food system decreased with increasing salt content (Fig. 4a). Based on the correlation between penetration depth and dielectric property (Von Von Hippel 1995), a significant increase of dielectric loss factor and small change in the dielectric constant with increasing salt content resulted in the significant decrease of penetration depths. Penetration depths generally increased with increasing sucrose content due to the decreased dielectric loss factor with increasing sucrose content (Fig. 4b). Accordingly, the penetration depth of new chemical marker-model food system could be well-adjusted by controlling the content of salt and sucrose.

Schiffmann (1995) recommended that the thickness of the processed food should not be larger than two or three times of the microwave penetration depth in dielectric heating to achieve a uniform heating. Therefore, the food ingredient, such as salt and sucrose, should be adjusted to allow a close match of the dielectric properties of the new model food system with the real foods in developing a microwave thermal process. The maximum penetration depths were around 30 mm with 0 mM salt and around 33 mm with 0.4 g/mL sucrose, which indicated that the maximum thickness of the new chemical marker-model food system in 915 MHz microwaves could be as high as approximately 90 and 100 mm correspondingly.

Texture Optimization of the New Chemical Marker-Model Food System

As previously described, a layer with 5 mm thickness needed to be cut horizontally below the middle plane of the model food for further analyses of heating pattern. Model foods with high strength and extensibility are required for better cutting for heating pattern determination. Tang et al. (1994) studied the failure stresses and strains of gellan gel under compressive, tensile, and torsional modes, and reported that shear stress was equal in the three modes, and proportional to gellan content; the shear strain decreased with the increasing Ca^{2+} concentration, and gellan gels were brittle with high Ca^{2+} concentration. Thus, high shear stress corresponded to high strength, while high shear strain reflected high extensibility of the gel system.

Our results showed that the shear strain of the new chemical marker-model food system decreased with Ca^{2+} concentration from 5 to 10 mM, then remained constant from 10 to 40 Mm. Higher shear strain of the system was obtained with 1.5% gellan at all Ca^{2+} concentrations (Fig. 5a). The shear stresses were first increased with Ca^{2+} concentration from 5 to 20 mM, then significantly decreased from 20 to 40 mM. The maximum shear stress was obtained with 1.5% gellan and 20 mM Ca^{2+} concentration (Fig. 5b).

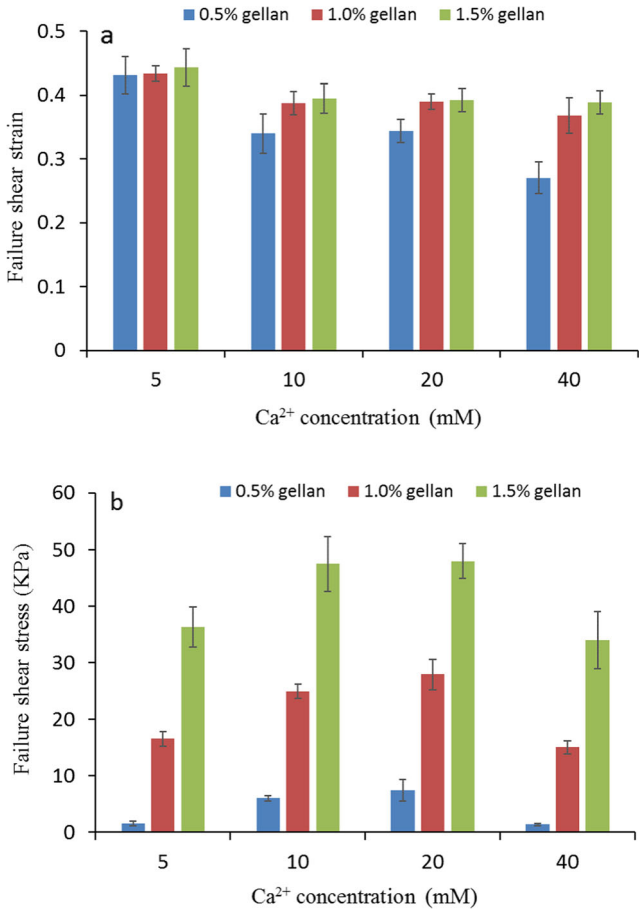

Fig. 5 Shear strain (**a**) and shear stress (**b**) at the failure of gellan gel with various gellan and Ca^{2+} concentration; mean ± SD for six determinations

An appropriate combination of gellan gum and cation concentration is required for the formation of a strong and clear gellan gel (Gibson and Sanderson 1997; Tang et al. 1995). The gelling mechanism started with forming double-helical junction zones, followed by direct cross-linking of cations to generate a stable gellan three-dimensional network (Chandrasekaran and Radha 1995). In the current study, both gellan gum and Ca^{2+} concentrations influenced the texture of gellan gel model food. Model food with 1.5% gellan gum had higher shear strains than 0.5 and 1% gellan gum and had the maximum shear stress with 20 mM Ca^{2+} among all the gel samples. Thus, 1.5% gellan gum was selected for the new chemical marker-model food system. For model foods with 1.5% gellan gum, 5 mM Ca^{2+} provided 11% higher shear strain but 24% lower shear stress than 10 and 20 mM Ca^{2+}. Thus, 10 and 20 mM Ca^{2+} were preferred to achieve high values of both the shear strain and stress. The shear strain and stress values were very similar of model foods with 10 and 20 mM Ca^{2+}; from the cost-saving perspective, 10 mM Ca^{2+} was selected as the optimal concentration for the new chemical marker-model food system.

Validation of the Heating Pattern in MAPS Process

After processing in MAPS, the heating pattern of the middle layer of new chemical marker-model food system in 10.5 oz tray was analyzed by CVS as shown in Fig. 6. The red color

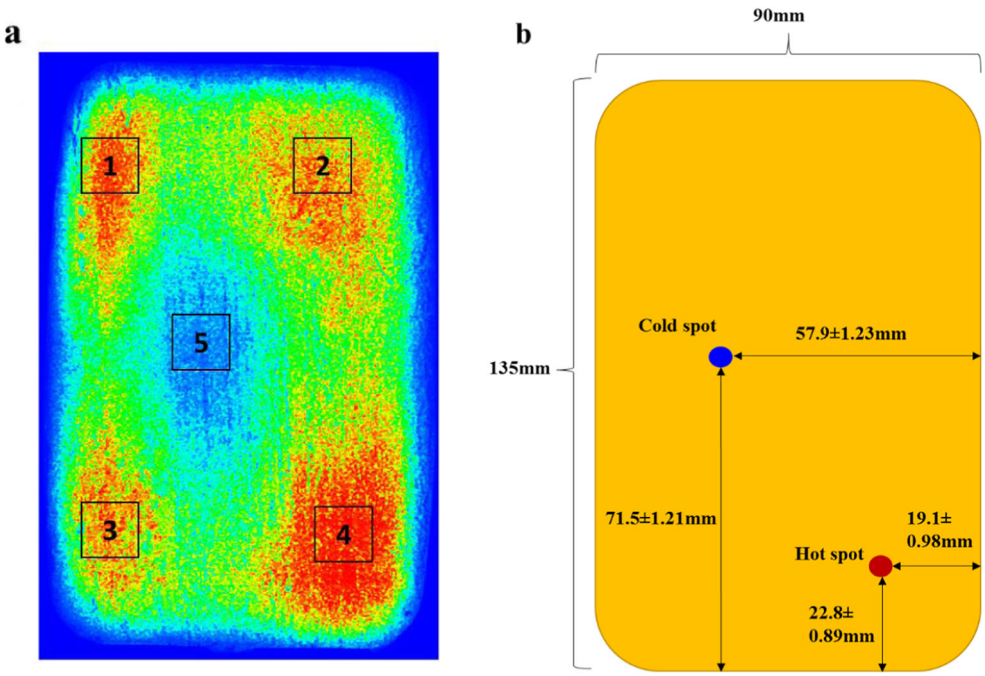

Fig. 6 Heating pattern (**a**) and cold/hot spot location (**b**) in 10.5-oz gellan gel model food tray of MAPS

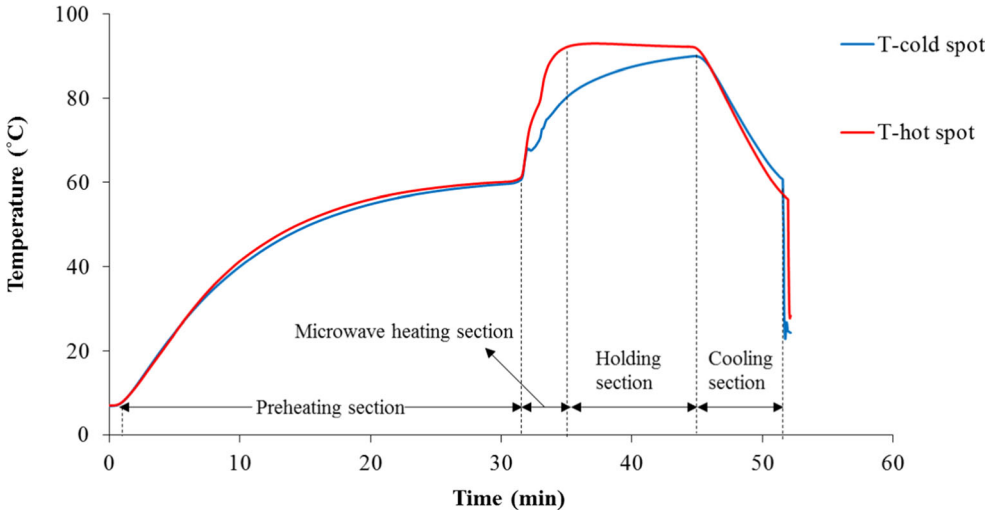

Fig. 7 Temperature profiles at the cold and hot spots in 10.5-oz gellan gel model food tray

corresponded to hot zones which received the most thermal energy, and the blue color corresponded to cold zones which received the least thermal energy. "Forward" represented the tray moving direction in MAPS. The CVS analysis results provided a clear heating pattern, in which four hot zones (Fig. 6a 1, 2, 3 and 4) and one cold zone (Fig. 6a 5) were represented visibly. Among the four hot zones, zone 4 had the highest red color concentration. Thus, the exact locations of the hot and cold spot were located in zones 4 and 5, respectively. The CVS then divided zones 4 and 5 into many small grids and confirmed the numeric locations of cold and hot spots (Fig. 6b) by comparing the color concentration of different grids in each zone.

Validation of cold and hot spots was conducted by inserting a TMI mobile metallic temperature sensor in the corresponding location (Luan et al. 2013). The complete temperature profiles of cold and hot spots in 10.5 oz tray during MAPS process are as shown in Fig. 7. The temperature of both cold and hot spots reached 60 °C after 30 min preheating, then the hot spot increased quickly to 90 °C, whereas the cold spot barely reached 80 °C in the microwave heating section. The temperature of hot spot stayed at 90 °C and the cold spot increased close to 90 °C after 6 min in holding section, then decreased together in the cooling section (cold spot F_{90} = 6.9 min). The temperature of the hot spot was consistently higher than the cold spot in the microwave heating and holding sections. Thus, the heating pattern detected from intensity of brown color formed in the new gellan gel system did allow detection of cold and hot spots in a MAPS.

Conclusions

A new chemical marker-model food system was developed for the heating pattern determination of the MAPS. Caramelization reaction (D-ribose and NaOH) was firstly used to produce brown color as the time-temperature indicator in model food system. The system is stable, low cost, easy to be prepared, and has high gel strength. Moreover, it can be adjusted to different levels of dielectric constant and loss factor to simulate various real foods. A clear heating pattern of the new chemical marker-model food system was obtained after processing in MAPS, and the locations of cold and hot spots were further validated. This work demonstrated that the new chemical marker-model food system provides clear and precise heating pattern of MAPS, which is required for process design to achieve reliable microbiological control after processing. The gellan gel system in this study was transparent, which might influence the heating pattern determination result. In the future study, additives such as titanium dioxide, modified starch, and milk powder are recommended to make the model food system opaque for more accurate heating pattern determination.

Acknowledgments This project was supported by Agriculture and Food Research Initiative of U.S. Department of Agriculture (Grant No. 2016-68003-24840). The authors also thank the Chinese Scholarship Council's support for his studies at Washington State University.

References

Ajandouz, E. H., & Puigserver, A. (1999). Nonenzymatic browning reaction of essential amino acids: effect of pH on caramelization and Maillard reaction kinetics. *Journal of Agricultural and Food Chemistry, 47*(5), 1786–1793.

Ajandouz, E. H., Tchiakpe, L. S., Ore, F. D., Benajiba, A., & Puigserver, A. (2001). Effects of pH on caramelization and Maillard reaction kinetics in fructose-lysine model systems. *Journal of Food Science, 66*(7), 926–931.

Ajandouz, E. H., Desseaux, V., Tazi, S., & Puigserver, A. (2008). Effects of temperature and pH on the kinetics of caramelisation, protein cross-linking and Maillard reactions in aqueous model systems. *Food Chemistry, 107*(3), 1244–1252.

Ashoor, S. H., & Zent, J. B. (1984). Maillard browning of common amino acids and sugars. *Journal of Food Science, 49*(4), 1206–1207.

Chandrasekaran, R., & Radha, A. (1995). Molecular architectures and functional properties of gellan gum and related polysaccharides. *Trends in Food Science and Technology, 6*(5), 143–148.

Chung, H. J., Wang, S., & Tang, J. (2007). Influence of heat transfer with tube methods on measured thermal inactivation parameters for Escherichia coli. *Journal of Food Protection, 70*(4), 851–859.

Espenson, J. H. (1995). *Chemical kinetics and reaction mechanisms (Vol. 102)*. New York: McGraw-Hill.

Gibson, W., & Sanderson, G. R. (1997). Gellan gum. In: *Thickening and gelling agents for food*. Boston: Springer.

Guan, D., Cheng, M., Wang, Y., & Tang, J. (2004). Dielectric properties of mashed potatoes relevant to microwave and radio-frequency pasteurization and sterilization processes. *Journal of Food Science, 69*, 30–37.

Hamann, D. D. (1983). Structure failure in solid foods. In M. Peleg & E. B. Bagley (Eds.), *Physical Properties of Foods* (pp. 351–383). Westport: AVI Publishing Inc..

Juvinall, R. C. (1967). *Engineering considerations of stress, strain, and strength (Vol. 66)*. New York: McGraw-Hill.

Kamuf, W., Nixon, A., Parker, O., & Barnum Jr., G. C. (2003). Overview of caramel colors. *Cereal Foods World, 48*(2), 64–69.

Kim, J. S., & Lee, Y. S. (2008). Effect of reaction pH on enolization and racemization reactions of glucose and fructose on heating with amino acid enantiomers and formation of melanoidins as result of the Maillard reaction. *Food Chemistry, 108*(2), 582–592.

Kim, H. J., & Taub, I. A. (1993). Intrinsic chemical markers for aseptic processing of particulate foods. *Food Technology, 47*(1), 91–97 99.

Kim, H. J., Taub, I. A., Choi, Y. M., & Prakash, A. (1996). *Principles and applications of chemical markers of sterility in high-temperature-short-time processing of particulate foods*. ACS Symposium Series, 631, Chapter 6, pp. 54–69.

Kuo, M. S., Mort, A. J., & Dell, A. (1986). Identification and location of L-glycerate, an unusual acyl substituent in gellan gum. *Carbohydrate Research, 156*, 173–187.

Lau, M. H., & Tang, J. (2002). Pasteurization of pickled asparagus using 915 MHz microwaves. *Journal of Food Engineering, 51*(4), 283–290.

Lau, H., Tang, J., Taub, I. A., Yang, T. C. S., Edwards, C. G., & Mao, R. (2003). Kinetics of chemical marker formation in whey protein gels for studying high temperature short rime microwave sterilization. *Journal of Food Engineering, 60*(4), 397–405.

Leon, K., Mery, D., Pedreschi, F., & Leon, J. (2006). Color measurement in L∗ a∗ b∗ units from RGB digital images. *Food Research International, 39*(10), 1084–1091.

Levinson, R. (2001). *More modern chemical techniques*. Piccadilly, London: Royal Society of Chemistry.

Luan, D., Tang, J., Pedrow, P. D., Liu, F., & Tang, Z. (2013). Using mobile metallic temperature sensors in continuous microwave assisted sterilization (MATS) systems. *Journal of Food Engineering, 119*(3), 552–560.

Luan, D., Tang, J., Pedrow, P. D., Liu, F., & Tang, Z. (2015a). Performance of mobile metallic temperature sensors in high power microwave heating systems. *Journal of Food Engineering, 149*, 114–122.

Luan, D., Tang, J., Liu, F., Tang, Z., Li, F., Lin, H., & Stewart, B. (2015b). Dielectric properties of bentonite water pastes used for stable loads in microwave thermal processing systems. *Journal of Food Engineering, 161*, 40–47.

Morris, E. R., Nishinari, K., & Rinaudo, M. (2012). Gelation of gellan—a review. *Food Hydrocolloids, 28*(2), 373–411.

Namiki, M. (1988). Chemistry of Maillard reactions: recent studies on the browning reaction mechanism and the development of antioxidants and mutagens. *Advances in Food Research, 32*, 115–184.

Pandit, R. B., Tang, J., Mikhaylenko, G., & Liu, F. (2006). Kinetics of chemical marker M-2 formation in mashed potato—a tool to locate cold spots under microwave sterilization. *Journal of Food Engineering, 76*(3), 353–361.

Pandit, R. B., Tang, J., Liu, F., & Pitts, M. (2007a). Development of a novel approach to determine heating pattern using computer vision and chemical marker (M-2) yield. *Journal of Food Engineering, 78*(2), 522–528.

Pandit, R. B., Tang, J., Liu, F., & Mikhaylenko, G. (2007b). A computer vision method to locate cold spot in foods during microwave sterilization processes. *Pattern Recognition, 40*(12), 3667–3676.

Pollock, T. J. (1993). Gellan-related polysaccharides and the genus Sphingomonas. *Journal of General Microbiology, 139*(8), 1939–1945.

Prakash, A., Kim, H. J., & Taub, I. A. (1997). Assessment of microwave sterilization of foods using intrinsic chemical markers. *Journal of Microwave Power and Electromagnetic Energy, 32*(1), 50–57.

Resurreccion, F. P., Tang, J., Pedrow, P., Cavalieri, R., Liu, F., & Tang, Z. (2013). Development of a computer simulation model for processing food in a microwave assisted thermal sterilization (MATS) system. *Journal of Food Engineering, 118*(4), 406–416.

Richardson, P. (Ed.). (2001). *Thermal technologies in food processing*. Cambridge: Woodhead Publishing.

Rizvi, A. F., & Tong, C. H. (1997). Fractional conversion for determining texture degradation kinetics of vegetables. *Journal of Food Science, 62*(1), 1–7.

Ryynänen, S. (1995). The electromagnetic properties of food materials: a review of the basic principles. *Journal of Food Engineering, 26*(4), 409–429.

Schiffmann, R. F. (1995). Microwave and dielectric drying. In A. S. Mujumdar (Ed.), *Handbook of Industrial Drying*. New York: Marcel Decker Inc 352 p.

Stogryn, A. (1971). Equations for calculating the dielectric constant of saline water (correspondence). *IEEE Transactions on Microwave Theory and Techniques, 19*(8), 733–736.

Stumbo, C. R. (1965). *Thermo-bacteriology in food processing*. New York: Academic Press Inc.

Tang, J. (2015). Unlocking potentials of microwaves for food safety and quality. *Journal of Food Science, 80*(8), 1776–1793.

Tang, J., Lelievre, J., Tung, M. A., & Zeng, Y. (1994). Polymer and ion concentration effects on gellan gel strength and strain. *Journal of Food Science, 59*(1), 216–220.

Tang, J., Tung, M. A., & Zeng, Y. (1995). Mechanical properties of gellan gels in relation to divalent cations. *Journal of Food Science, 60*(4), 748–752.

Tang, J., Tung, M. A., & Zeng, Y. (1997a). Gelling temperature of gellan solutions containing calcium ions. *Journal of Food Science, 62*(2), 276–280.

Tang, J., Tung, M. A., & Zeng, Y. (1997b). Gelling properties of gellan solutions containing monovalent and divalent cations. *Journal of Food Science, 62*(4), 688–692,712.

Tang, J., Mao, R., Tung, M. A., & Swanson, B. G. (2001). Gelling temperature, gel clarity and texture of gellan gels containing fructose or sucrose. *Carbohydrate Polymers, 44*(3), 197–209.

Tang, Z., Mikhaylenko, G., Liu, F., Mah, J. H., Tang, J., Pandit, R., & Younce, F. (2008). Microwave sterilization of sliced beef in gravy in 7-oz trays. *Journal of Food Engineering, 89*(4), 375–383.

Thorne, S. (1986). *The history of food preservation*. New York City: Barnes and Noble Books.

To, E. C., Mudgett, R. E., Wang, D. I. C., Goldblith, S. A., & Decareau, R. V. (1974). Dielectric properties of food materials. *Journal of Microwave Power, 9*(4), 303–315.

Tran, V. N., & Stuchly, S. S. (1987). Dielectric properties of beet, beer liver, chicken and salmon at frequencies from 100 to 2500 MHz. *Journal of Microwave Power and Electromagnetic Energy, 22*(1), 29–33.

Venkatesh, M. S., & Raghavan, G. S. V. (2004). An overview of microwave processing and dielectric properties of agri-food materials. *Biosystems Engineering, 88*(1), 1–18.

Von Hippel, A. R. (1995). *Dielectric and waves*. Norwood: Artech House. Inc.

Wang, S., Tang, J., Johnson, J. A., Mitcham, E., Hansen, J. D., Hallman, G., & Wang, Y. (2003a). Dielectric properties of fruits and insect pests as related to radio frequency and microwave treatments. *Biosystems Engineering, 85*(2), 201–212.

Wang, Y., Wig, T., Tang, J., & Hallberg, L. (2003b). Dielectric properties of foods related to RF and microwave pasteurization and sterilization. *Journal of Food Engineering, 57*(3), 257–268.

Wang, Y., Lau, M. H., Tang, J., & Mao, R. (2004). Kinetics of chemical marker M-1 formation in whey protein gels for developing sterilization processes based on dielectric heating. *Journal of Food Engineering, 64*(1), 111–118.

Wang, S., Monzon, M., Gazit, Y., Tang, J., Mitcham, E. J., & Armstrong, J. W. (2005). Temperature-dependent dielectric properties of selected subtropical and tropical fruits and associated insect pests. *Transactions of the American Society of Agricultural Engineers, 48*(5), 1873–1881.

Zhang, W., Liu, F., Nindo, C., & Tang, J. (2013). Physical properties of egg whites and whole eggs relevant to microwave pasteurization. *Journal of Food Engineering, 118*(1), 62–69.

Zhang, W., Tang, J., Liu, F., Bohnet, S., & Tang, Z. (2014). Chemical marker M2 (4-hydroxy-5-methyl-3 (2H)-furanone) formation in egg white gel model for heating pattern determination of microwave-assisted pasteurization processing. *Journal of Food Engineering, 125*, 69–76.

Zhang, W., Luan, D., Tang, J., Sablani, S. S., Rasco, B., Lin, H., & Liu, F. (2015). Dielectric properties and other physical properties of low-acyl gellan gel as relevant to microwave assisted pasteurization process. *Journal of Food Engineering, 149*, 195–203.

Zimeri, J., & Tong, C. H. (1999). Degradation kinetics of (−)-epigallocatechin gallate as a function of ph and dissolved oxygen in a liquid model system. *Journal of Food Science, 64*(5), 753–758.